Journal of Medical Imaging & Case Reports

https://doi.org/10.17756/micr.2020-050

Research Article

Open Access

The Pulmonary Venous Ridge Length to Stratify Stroke Risk in Atrial Fibrillation

Varun Singh[1*], Joy Li[1], Mark Keroles[1], Daniel Frisch[2], Behzad B. Pavri[2], Baskaran Sundaram[3], Jason Jacobson[4] and Rajiv Kabadi[2]

[1]*Sidney Kimmel Medical College of Thomas Jefferson University, Philadelphia, PA, USA*
[2]*Department of Medicine, Division of Cardiology, Thomas Jefferson University, Philadelphia, PA, USA*
[3]*Department of Radiology, Thomas Jefferson University, Philadelphia, PA, USA*
[4]*Department of Cardiology, Westchester Medical Center Health, Philadelphia, PA, USA*

[*]Correspondence to:
Dr. Varun Singh, MD
Department of Radiology
Thomas Jefferson University
901 Walnut St. Philadelphia
PA 19107, USA
E-mail: varun.singh@jefferson.edu

Received: March 04, 2020
Accepted: June 29, 2020
Published: July 01, 2020

Citation: Singh V, Li J, Keroles M, Frisch D, Pavri B, et al. 2020. The Pulmonary Venous Ridge Length to Stratify Stroke Risk in Atrial Fibrillation. *J Med Imaging Case Rep* 4(2): 48-53.

Published by United Scientific Group

Abstract

Purpose of Study: To evaluate the left superior pulmonary venous ridge length (RL) and the left atrial appendage fractal dimension (LAA FD) as predictors of cardioembolic ischemic stroke (CVA) and transient ischemic attack (TIA) in patients with atrial fibrillation (AF).

Materials, Methods and Procedures: A multicenter, retrospective multi-center study was conducted on patients with AF who underwent cardiac CT prior to catheter ablation between 01/01/2010 and 12/31/2015. Patients were grouped by presence or absence of prior CVA/TIA. Patients with mitral stenosis, prior mechanical aortic valve replacement, ascending aortic arch atheroma, high-risk patent foramen ovale, history of atrial septal repair or device, preexisting LAA thrombus or intra-cardiac tumor, or prior open-heart surgery were excluded. Further exclusion was performed for patients with sub-optimal or unavailable cardiac CT imaging by investigators blinded to clinical data. Blinded investigators obtained RL by measuring the distance between the left superior pulmonary venous ostium and the internal ostium of the left atrial appendage. LAA FD was calculated using semi-automated volume rendering and processing software (ImageJ, Bethesda, MD) [1] and LAA FD are presented as means (95% confidence interval) and were compared between groups using unpaired t-tests. Logistic regression analysis was used to construct receiver operating curves and to assess the abilities of RL and LAA FD to predict prior CVA/TIA.

Results: 225 patients met inclusion criteria. Mean RL were 4.32 (3.80-4.93) and 5.20 (4.93-5.48) for patients with (n=24; mean age: 59.4; 70.8% male) and without (n=165; mean age: 59.3; 75.4% male) prior CVA/TIA, respectively (p=0.033). Mean LAA FD were 2.29 (95% CI: 2.24-2.34) and 2.33 (2.32-2.34) for patients with (n=22; mean age: 60.3; 68.2% male) and without (n=171; mean age: 59.3; 74.9% male) prior CVA/TIA, respectively (p=0.052). In a regression model including LAA FD, RL, and established predictive markers, only RL predicted prior CVA/TIA (OR 0.73; 0.54 to 0.98; p=0.034).

Discussion: Lower RL values were associated with prior CVA/TIA, whereas LAA FD values were similar between patients with AF with and without prior CVA/TIA. RL is a novel marker that may refine clinical decision-making regarding anticoagulation goals and treatment decisions for patients with AF. Future studies with larger samples should investigate the clinical utility of RL to improve CVA/TIA risk stratification of patients with AF and prospectively reduce the incidence of CVA/TIA in this population.

Keywords

Atrial fibrillation, Left atrial appendage, Stroke, CVA, Ridge length

Introduction

The mechanism of cardioembolic ischemic stroke (CVA) in atrial fibrillation (AF) is well-validated. Among patients with AF, left atrial thromboembolism is the mechanism underlying CVA in approximately 70% of cases [2] with up to 90% of these specifically originating from the left atrial appendage (LAA) based on autopsy and radiographic studies [3].

Therapeutic anticoagulation is the principle strategy used to prevent CVA in patients with AF deemed to be at increased risk. The decision to treat is primarily informed by a validated clinical decision-making tool known as the CHA_2DS_2-VASc scoring system to estimate an individual patient's annual risk of CVA based on the presence of certain risk factors (heart failure, hypertension, age, diabetes mellitus, vascular disease, female gender). A CHA_2DS_2-VASc score of 2 or greater is considered an indication to initiate therapeutic anticoagulation in most patients whereas a score of 0 indicates low-dose aspirin monotherapy [2-3]. While well-validated in high-risk populations, large retrospective meta-analyses have reported poor predictive value for intermediate-risk patients, or patients with CHA_2DS_2-VASc scores of 1 [4, 5]. CHA_2DS_2-VASc scores are similarly imprecise in identifying high-risk patients who would receive net clinical benefit from long-term anticoagulation [4, 5].

Radiographic LAA structural parameters have previously been studied to predict CVA/TIA among patients with AF. LAA volume has long been considered an independent marker of thromboembolic risk in AF [6-8]. Additionally, patients with suspected cardioembolic CVA often demonstrated increased LAA volume and single-lobed LAA morphology [9].

Retrospective studies have identified archetypal LAA morphologies (Figure 1) derived from cross-sectional imaging and assessed their role in predicting CVA risk in patients with AF. Di Biase and colleagues reported a negative association between CVA risk and presence of the 'chicken wing' LAA morphology that persisted when controlling for other risk factors in multivariate analysis [10]. One study attributed the higher risk 'chicken wing morphology' to higher maximal LAA empty flow velocity [11]. Significant data heterogeneity and imprecision have been cited as major limitations to this approach to studying LAA morphology [12].

In figure 1, the four originally described archetypal LAA morphologies volume-rendered and segmented from cardiac computed tomographic angiographic (CCTA) studies. LAA reconstructions are designated as windsock, chicken wing, broccoli, and cactus morphologies (left to right). Retrospective studies have associated lower risk of CVA with presence of the chicken wing LAA morphology [10].

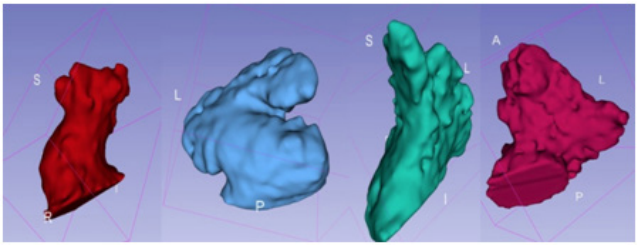

Figure 1: Volume-rendered LAA segmentations (left to right): Wind sock morphology, chicken wing morphology, broccoli morphology, and cactus morphology.

Fractal dimensions (FD) are ratios that provide statistical indices of complexity by measuring how the complexity of each object varies with each measuring scale. FDs have been applied to study heterogeneous biological objects derived from radiographic and histologic modalities where they have been shown to yield highly reproducible and accurate data [13]. To the best of our knowledge, the present study is the first attempt to apply fractal analysis to evaluate the role of LAA morphology in CVA risk among patients with AF and to stratify stroke risk in AF. We hypothesize that a higher FD reflects a more complex or irregularly structured LAA endocardial surface that is more likely to produce abnormal blood flow and serve as a nidus for thromboembolism. Therefore the LAA FD may be a clinically useful marker of CVA risk in patients with AF.

The relationships between the LAA and other atrial features have been investigated as predictors of thromboembolism in atrial fibrillation [14-22]. LAA "take-off" was defined by Nedios et al. as whether the superior and inferior LAA ostial ridges were "higher" or "lower" than the respective left superior pulmonary vein (LSPV) and the right superior pulmonary vein (RSPV) [17]. Nedios et al. proposed a pathophysiologic mechanism of tachycardia-mediated thrombogenic flow in patients with superior LAA "takeoff" anatomy, and that inferior LAA "takeoff" anatomy is protective against cardioembolic events in AF [17]. Electrophysiologists at [institution blinded] observed variation in both size and thickness of the ridge of tissue interfacing between the LSPV and the LAA upon review of CCTA studies prior to catheter-based ablation procedures. A systematic literature review demonstrated no prior studies attempting to classify or investigate this structure, and the pulmonary venous ridge length (RL) is proposed as the designation of the interface between the LSPV and the LAA.

The purpose of this study is to investigate the abilities of the LAA FD and RL to predict CVA and/or transient ischemic attack (TIA) in patients with AF.

Methods

A multicenter, retrospective study was performed using patients with AF who underwent both cardiac CT and catheter ablation between 01/01/2010 and 12/31/2015. 205 patients from [institution blinded] and 20 patients from [institution blinded] were stratified based on the presence or

absence of prior CVA/TIA.

Exclusion was performed based on the presence of mitral stenosis, prior mechanical aortic valve replacement, ascending aortic arch atheroma, high risk patent foramen ovale, history of atrial septal repair or device, preexisting LAA thrombus, intracardiac tumor, or prior open-heart surgery. Independent investigators blinded to radiographic data completed a retrospective chart review for the cohort, obtaining baseline characteristics of age, patient sex, and CHA_2DS_2-VASc scores. Corresponding patient CCTA studies were de-identified and randomized, and further exclusion was performed on the basis of study availability by investigators blinded to clinical data.

Open-source image processing with volume-rendering software was utilized (3D Slicer [23]) to analyze CCTA studies. On three-view analysis (coronal, sagittal, and axial), manual binary selection of cardiac blood pool and non-contrast phases was performed (Figure 2). A native automated thresholding function for total binarization was then applied, and a cropped three-dimensional volume was rendered following manual cropping by trained investigators at the level of each LAA ostium.

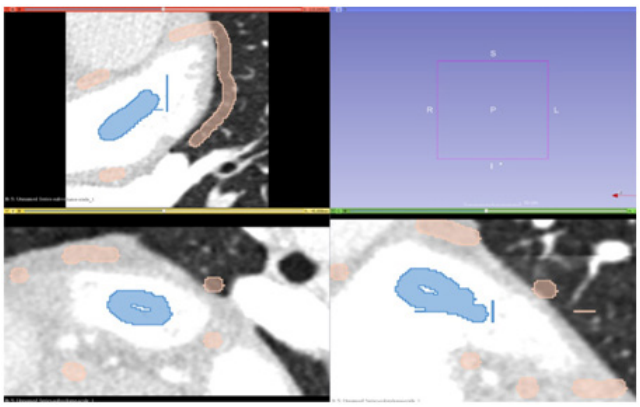

Figure 2: Three-view view of CCTA study for binarization and semi-automated LAA segmentation.

Following the generation of a cropped volume and three-dimensional model, volumes were saved as NRRD files that were imported into a custom batch processor (Figure 3) leveraging an open source fractal analysis algorithm and Image J (NIH [1]) to compute LAA FDs for each segmentation.

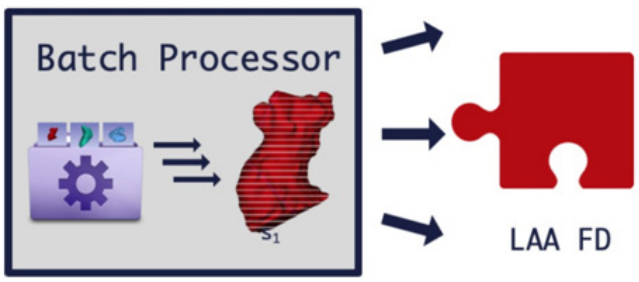

Figure 3: Batch processor schematic of LAA segmentations to generate LAA FD values.

Schematic depicting the batch-processing algorithm we developed and utilized to generate LAA FD values (Figure 3). Two-dimensional metrics were instantly compiled using custom-designed running summation, average, and standard deviation scripts.

The native measurement tool from the open-source image processing software (3D Slicer [23]) was utilized to measure RL from CCTA studies. RL was measured on axial CCTA section as the shortest distance (width) perpendicular to the vector direction of the ridge wall extending between the LSPV and the LAA (Figures 4-9). Two board-certified electrophysiologists and one board-certified cardiothoracic radiologist measured RL. Ground truth labels were determined

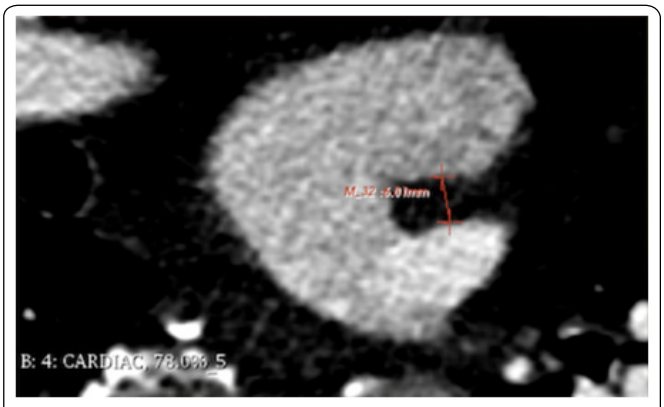

Figure 4: RL measurement derived from CCTA measuring shortest length (mm) from the LAA to the LSPV perpendicular to axis of the pulmonary venous ridge (RL=6.01).

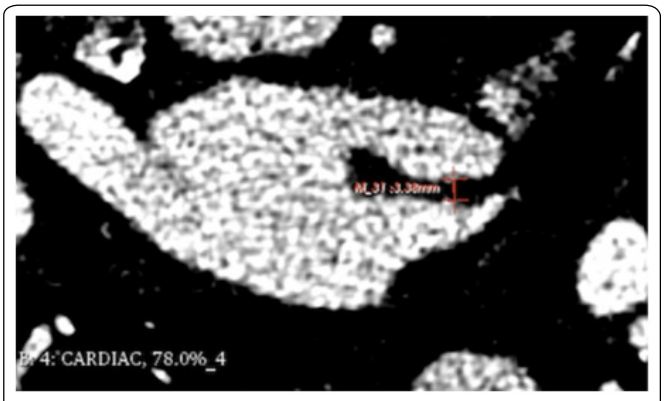

Figure 5: RL=3.38 in a patient with prior CVA.

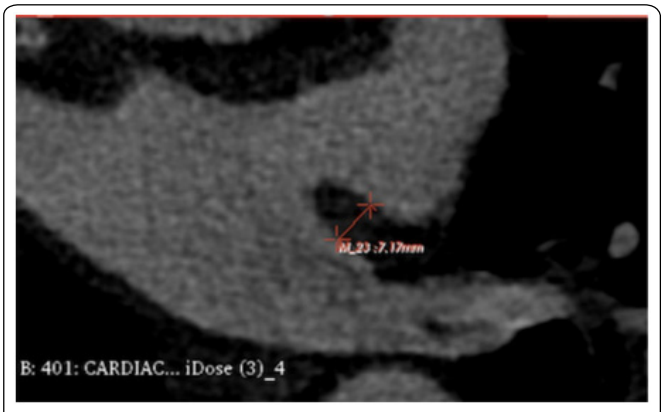

Figure 6: RL=7.17 in a patient with no prior CVA.

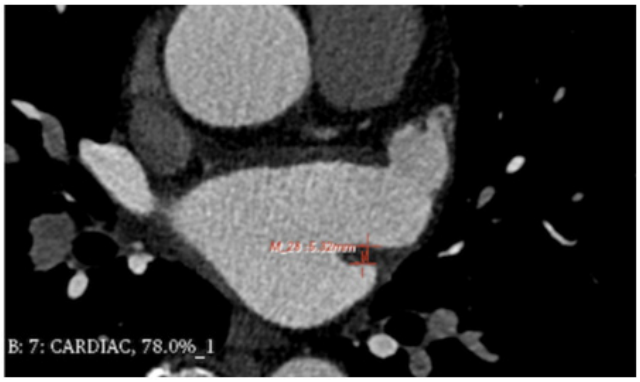

Figure 7: RL=5.32 in a patient with no prior CVA.

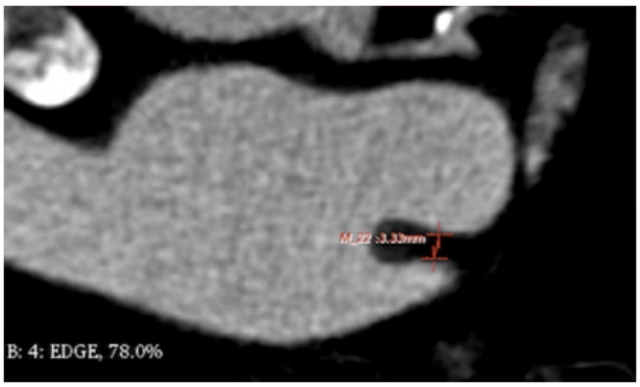

Figure 8: RL=3.33 in a patient with no prior CVA.

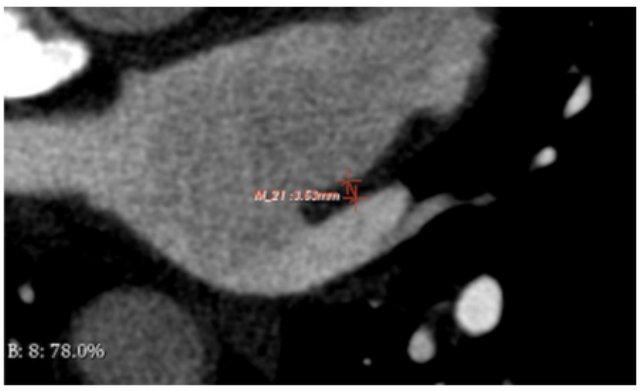

Figure 9: RL=3.53 in a patient with no prior CVA.

by mean RLs with consensus measurements. Inter-rater variability was not formally statistically evaluated.

Statistical analyses were performed using Prism 6 (GraphPad Software, San Diego, CA). The unpaired student's t-test was used to compare continuous variables. Multivariate logistic regression analysis was used to identify clinical variables predictive of prior CVA/TIA. Classifier values were assessed through receiver operating characteristic analysis to calculate the area-under- the-curve.

Results

Significantly fewer subjects had histories of CVA/TIA compared to those without. Baseline study cohort characteristics were otherwise similar (Table 1). Mean RL were 4.32 (3.80-4.93) and 5.20 (4.93-5.48) for patients with (n=24; mean age: 59.4; 70.8% male) and without (n=165; mean age: 59.3; 75.4% male) prior CVA/TIA, respectively (p=0.033). Mean LAA FD were 2.29 (95% CI: 2.24-2.34) and 2.33 (2.32-2.34) for patients with (n=22; mean age: 60.3; 68.2% male) and without (n=171; mean age: 59.3; 74.9% male) prior CVA/TIA, respectively (p=0.052). In a regression multivariate analysis model including LAA FD, RL, CHA_2DS2-VASc scores, and individual CHA_2DS_2-VASc scoring criteria, only RL was a significant predictor of prior CVA/TIA (OR 0.73; 0.54 to 0.98; p=0.034) (Table 2).

Table 1: Study cohort characteristics.

	LAA FD		RL	
	Past CVA/TIA n = 22	No Past CVA/TIA n = 171	Past CVA/TIA n = 24	No Past CVA/TIA n = 175
Male, No. (%)	15 (68.2)	128 (74.9)	17 (70.8)	132 (75.4)
Age, mean (SD)	60.3 (10.1)	59.3 (10.3)	59.4 (10.6)	59.3 (9.9)
Median CHA_2DS_2-VASc Score*	2 (1 to 3)	2 (1 to 2)	1.5 (1 to 3)	1 (1 to 3)
Median CHA_2DS_2-VASc Score* (Interquartile Range)	2 (1 to 3)	2 (1 to 2)	1.5 (1 to 3)	1 (1 to 3)

Discussion

A lower RL predicted prior CVA/TIA in patients with AF whereas LAA FD was similar between patients with and without prior CVA/TIA.

Our findings serve as proof-of-concept for the semi-automated workflow developed and utilized to segment anatomic structures of interest from standard-of-care cross-

Table 2: LAA FD and RL values and results of statistical analysis (significance defined at $\alpha < 0.05$).

	Mean (95% CI)						
	Past CVA/TIA	No Past CVA/TIA	P-Value for Comparison	Odds Ratio (95% CI)	P-Value for Regression	Area under the curve (AUC)	P-Value for AUC = 0.5
LAA FD	2.292	2.326	0.0519	0.004	0.0548	0.59	0.2322
	(2.243 to 2.341)	(2.315 to 2.337)		(0.000 to 1.119)		(0.517 to 0.660)	
RL	4.319	4.319	0.033	0.727	0.0342	0.635	0.0168
	(3.796 to 4.842)	(4.861 to 5.393)		(0.541 to 0.977)		(0.564 to 0.702)	

sectional imaging. Custom fractal analysis batch-processing soft-ware derived from ImageJ (NIH [1]) created for this investigation provides a scalable approach for volumetric analysis from large datasets.

RL values were significantly lower in patients with prior CVA/TIA and represented the only statistically significant parameter in multivariate logistic regression analysis incorporating LAA FD and individual parameters from the CHA_2DS_2-VASc scoring system. RL measurements involved two-dimensional measurements between two iodinated structures and were less work-intensive and less sensitive to variations in study quality, in comparison to LAA FD calculations which depended upon three-dimensional volumetric analysis. Furthermore, RL is feasible to obtain using native measurement tools from standard-of- care medical imaging digital access platforms such as the PACS and therefore can be efficiently reported by radiologists in CCTA study reports. Subjective investigator assessments of perpendicular axes to each pulmonary venous ridge and the shortest distances between the LAA and LSPV represent possible sources of variation that should be considered in interpreting such data. In this study, ground-truth RL measurements were determined by statistical means from observers and consensus.

Variations in RL may play a potential role in thrombogenic flow within the LAA. The possible presence of muscular bands or trabeculated surface irregularity within the pulmonary venous ridge could also result in higher risk for thrombus formation and subsequent thromboembolism. If RL is shown to be a useful marker for thromboembolic risk in AF, then it could be utilized for clinical scoring and to direct treatment in AF.

Additional feasibility studies are warranted to further assess clinical benefit and efficacious value-based resource utilization of the time radiologists would spend during manual semi-automated segmentation of the LAA to ultimately obtain the LAA FD. The role of machine learning and fully convoluted neural networks (FCNs) could provide an automated, validated solution to LAA segmentation from CCTA, as FCNs have already demonstrated success in the segmentation of pancreatic structures on CT [24].

Nedios et al., proposed "tachycardiac-mediated thrombogenic flow" as a possible mechanism for increased thromboembolic risk in patients with higher LAA "takeoff" with respect to the LSPV and LIPV [16]. If our findings are confirmed in larger prospective studies, future studies should investigate differential patterns of left atrial blood flow in AF as RL varies through use of modalities such as Doppler echocardiography and four-dimensional flow MRI to identify a pathophysiologic thromboembolic mechanism [25]. Electrophysiological analyses of the conductive features of the pulmonary venous ridge may also be helpful to assess for the presence of muscular bands or arrhythmogenic foci with variant activation frequency within the pulmonary venous ridge.

Current clinical scoring criteria using the CHA_2DS_2-VASc demonstrates modest efficacy in appropriately indicating anticoagulation therapy in AF [5]. The P2-CHA_2DS_2-VASc score has been validated as an improved scoring criterion for stroke risk in AF by incorporating abnormal p-wave axis from prothrombotic atrial remodeling in stroke risk as an additional index for the administration of anticoagulation [26]. The primary clinical application of RL would be to identify patients with AF at increased CVA risk to achieve early initiation of therapeutic anticoagulation. Larger studies and further investigation of the pathophysiologic mechanisms underlying LA thromboembolism in AF related to the RL are necessary to clarify the utility of the RL to inform clinical decision-making.

Our relatively small sample size of patients with prior CVA/TIA and the overall precision of the LAA FD values obtained render meaningful interpretation of our findings difficult. The non-significant trend observed in these data would suggest that a lower LAA FD is associated with prior CVA/TIA, which contrasts with our initial hypothesis and established pathophysiologic mechanisms of cardioembolic CVA [7]. Variations in CCTA study quality and contrast dose imposed artifact and spiculation into the semi-automated volume-rendering LAA segmentations. The incorporation of variable artifact and spiculation from CCTA studies constitutes a confounding variable affecting the internal validity of the LAA FD data. The manual cropping of LAA ostia during semi-automated volume rendering additionally incorporates a subjective component, which also threatens the validity of these findings. Based on these findings, the authors conclude that larger studies are necessary to clarify the role of the LAA FD to predict CVA/TIA in AF.

Conclusion

LAA FD and RL are novel parameters derived from standard-of-care CCTA imaging with potential utility to refine clinical decision-making for patients with AF. In this retrospective study, LAA FD values were similar between patients with AF with and without prior CVA/TIA, whereas a lower RL predicted prior CVA/TIA. These parameters should be further investigated in larger and prospective studies to clarify their utilities in refining clinical decision-making for intermediate-risk patients with AF. In addition, future studies should clarify possible pathophysiologic mechanisms related to RL and LA thrombosis.

Conflict of Interest

The authors declared no conflict of interest.

References

1. P. Henden, R. Domander. 2012. Image J Fractal Dimension. Perchrh/ ImageFractalDimension https://github.com/ perchrh/Image J Fractal Dimension
2. Pollick C, Taylor D. 1991. Assessment of left atrial appendage function by transesophageal echocardiography. Implications for the development

of thrombus. *Circulation* 84(1): 223-231. https://doi.org/10.1161/01.cir.84.1.223

3. Blackshear JL, Odell JA. 1996. Appendage obliteration to reduce stroke in cardiac surgical patients with atrial fibrillation. *Ann Thorac Surg* 61(2): 755-759. https://doi.org/10.1016/0003-4975(95)00887-X
4. Karthikeyan G, Eikelboom JW. 2010. The $CHADS_2$ score for stroke risk stratification in atrial fibrillation--friend or foe? *Thromb Haemost* 104(1): 45-48. https://doi.org/10.1160/th09-11-0757
5. Van Staa TP, Setakis E, Di Tanna GL, Lane DA, Lip GYH. 2011. A comparison of risk stratification schemes for stroke in 79,884 atrial fibrillation patients in general practice. *J Thromb Haemost* 9(1): 39-48. https://doi.org/10.1111/j.1538-7836.2010.04085.x
6. Somerville WR, Chambers RJ. 1964. Systemic embolism in mitral stenosis: relation to the size of the left atrial appendix. *Br Med J* 2(5418): 1167-1169. https://doi.org/10.1136/bmj.2.5418.1167
7. Ernst G, Stöllberger C, Abzieher F, Veit-Dirscher W, Bonner E, et al. 1995. Morphology of the left atrial appendage. *Anat Rec* 242(4): 553-561. https://doi.org/10.1002/ar.1092420411
8. Veinot JP, Harrity PJ, Gentile F, Khandheria BK, Bailey KR, et al. 1997. Anatomy of the normal left atrial appendage: a quantitative study of age-related changes in 500 autopsy hearts: implications for echocardiographic examination. *Circulation* 96(9): 3112-3115. https://doi.org/10.1161/01.cir.96.9.3112
9. Korhonen M, Muuronen A, Arponen O, Mustonen P, Hedman M, et al. 2015. Left atrial appendage morphology in patients with suspected cardiogenic stroke without known atrial fibrillation. *PLoS One* 10(3): e0118822. https://doi.org/10.1371/journal.pone.0118822
10. Di Biase L, Santangeli P, Anselmino M, Mohanty P, Salvetti I, et al. 2012. Does the left atrial appendage morphology correlate with the risk of stroke in patients with atrial fibrillation? results from a multicenter study. *J Am Coll Cardiol* 60(6):531-538. https://doi.org/10.1016/j.jacc.2012.04.032
11. Petersen M, Roehrich A, Balzer J, Shin DI, Meyer C, et al. 2015. Left atrial appendage morphology is closely associated with specific echocardiographic flow pattern in patients with atrial fibrillation. *Europace* 17(4): 539-545. https://doi.org/10.1093/europace/euu347
12. Kimura T, Takatsuki S, Inagawa K, Katsumata Y, Nishiyama T, et al. 2013. Anatomical characteristics of the left atrial appendage in cardiogenic stroke with low CHADS2 scores. *Heart Rhythm* 10(6): 921-925. https://doi.org/10.1016/j.hrthm.2013.01.036
13. Michallek F, Dewey M. 2014. Fractal analysis in radiological and nuclear medicine perfusion imaging: a systematic review. *Eur Radiol* 24(1): 60-69. https://doi.org/10.1007/s00330-013-2977-9
14. Beinart R, Heist EK, Newell JB, Holmvang G, Ruskin JN, et al. 2011. Left atrial appendage dimensions predict the risk of stroke/TIA in patients with atrial fibrillation. *J Cardiovasc Electrophysiol* 22(1): 10-15. https://doi.org/10.1111/j.1540-8167.2010.01854.x
15. Burrell LD, Horne BD, Anderson JL, Muhlestein JB, Whisenant BK, et al. 2013. Usefulness of left atrial appendage volume as a predictor of embolic stroke in patients with atrial fibrillation. *Am J Cardiol* 112(8): 1148-1152. https://doi.org/10.1016/j.amjcard.2013.05.062
16. Nedios S, Koutalas E, Kornej J, Rolf S, Arya A, et al. 2015. Cardiogenic stroke despite low CHA_2DS_2-VASc Score: assessing stroke risk by left atrial appendage anatomy. *J Cardiovasc Electr* 26(9): 915-921. https://doi.org/10.1111/jce.12749
17. Nedios S, Kornej J, Koutalas E, Bertagnolli L, Kosiuk J, et al. 2014. Left atrial appendage morphology and thromboembolic risk after catheter ablation for atrial fibrillation. *Heart Rhythm* 11(12): 2239-2246. https://doi.org/10.1016/j.hrthm.2014.08.016
18. Anselmino M, Scaglione M, Di Biase L, Gili S, Santangeli P, et al. 2014. Left atrial appendage morphology and silent cerebral ischemia in patients with atrial fibrillation. *Heart Rhythm* 11(1): 2-7. https://doi.org/10.1016/j.hrthm.2013.10.020
19. Lacomis JM, Goitein O, Deible C, Moran PL, Mamone G, et al. 2007. Dynamic multidimensional imaging of the human left atrial appendage. *Europace* 9(12): 1134-1140. https://doi.org/10.1093/europace/eum227
20. Khurram IM, Dewire J, Mager M, Maqbool F, Zimmerman SL, et al. 2013. Relationship between left atrial appendage morphology and stroke in patients with atrial fibrillation. *Heart Rhythm* 10(12): 1843-1849. https://doi.org/10.1016/j.hrthm.2013.09.065
21. Koplay M, Erol C, Paksoy Y, Kivrak AS, Ozbek S. 2012. An investigation of the anatomical variations of left atrial appendage by multidetector computed tomographic coronary angiography. *Eur J Radiol* 81(7): 1575-1580. https://doi.org/10.1016/j.ejrad.2011.04.060
22. Park HC, Shin J, Ban JE, Choi JI, Park SW, et al. 2013. Left atrial appendage: morphology and function in patients with paroxysmal and persistent atrial fibrillation. *Int J Cardiovasc Imaging* 29(4): 935-944. https://doi.org/10.1007/s10554-012-0161-y
23. Kikinis R, Pieper SD, Vosburgh KG. 2014. 3D slicer: a platform for subject-specific image analysis, visualization, and clinical support. In: Jolesz F (eds) Intraoperative Imaging and Image-Guided Therapy. Springer, New York, pp 277-289. https://doi.org/10.1007/978-1-4614-7657-3_19
24. Roth HR, Lu L, Farag A, Shin HC, Liu J, et al. 2015. DeepOrgan: multi-level deep convolutional networks for automated pancreas segmentation. In: Navab N, Hornegger J, Wells W, Frangi A (eds) Medical Image Computing and Computer-Assisted Intervention -- MICCAI 2015. Lecture Notes in Computer Science, Springer, pp 556–564. https://doi.org/10.1007/978-3-319-24553-9_68
25. van der Geest RJ, Garg P. 2016. Advanced analysis techniques for intracardiac flow evaluation from 4D flow MRI. *Curr Radiol Rep* 4: 38. https://doi.org/10.1007/s40134-016-0167-7
26. Maheshwari A, Norby FL, Roetker NS, Soliman EZ, Koene RJ, et al. 2019. Refining prediction of atrial fibrillation-related stroke using the P_2-CHA_2DS_2-VASc score. *Circulation* 139(2): 180-191. https://doi.org/10.1161/circulationaha.118.035411